Real-Time Rail Energy Consumption Minimization: Optimal Speed Profile Planning

1st László Lindenmaier
Dept. of Control for Transportation and Vehicle Systems
Budapest University of Technology and Economics
Budapest, Hungary
lindenmaier.laszlo@kjk.bme.hu

2nd Szilárd Aradi
Dept. of Control for Transportation and Vehicle Systems
Budapest University of Technology and Economics
Budapest, Hungary
aradi.szilard@kjk.bme.hu

3rd István Ferenc Lövétei
Dept. of Control for Transportation and Vehicle Systems
Budapest University of Technology and Economics
Budapest, Hungary
lovetei.istvan@kjk.bme.hu

***Abstract*—In rail traffic, the timetable must be re-planned in real-time when traffic is perturbed. Methods that optimally reroute and reschedule the trains to resolve this traffic management problem already exist. These optimization models usually focus on minimizing delays. However, energy consumption is a key to economical and sustainable transportation. In this paper, we propose a method that calculates optimal speed profiles to minimize the energy consumption of the trains after solving the rerouting and rescheduling problems with a conventional model. Using a simulation environment, the proposed method is evaluated in two different rail networks. According to the experimental results, the proposed model can decrease the overall energy consumption by more than 10% on average.**

***Index Terms*—Rail transportation, Railway engineering, Optimization, Energy consumption, Minimization**

I. Introduction

Rail transportation has the most favorable specific energy consumption and the highest passenger load factor compared to other means of road transport [1], [2]. Therefore, rail services will have a higher role in future transportation [3]–[5]. An energy-efficient operation can significantly decrease rail transportation costs and contribute to reaching the global CO_2 emission targets. Many energy optimization forms and levels of rail transportation exist [6]. There are two main branches of railway energy consumption optimization: energy-efficient train control (EETC) and energy-efficient train timetabling (EETT) [7]. EETC aims to minimize the traction energy of a train, given its timetable, using the combination of the four optimal driving regimes [8]: maximum acceleration, maximum deceleration, coasting, and cruising, as in [9]–[11]. The energy consumption is usually formulated according to two principles. Most of these works, as [12]–[14], rely on the Davis equation that models the air drag resistance. Others consider the trains as mass points and formulate the problem according to the Maximum Principle [15], [16]. Various optimization methods also exist, such as mixed integer linear programming (MILP) [17], genetic algorithm (GA) [18], ant colony optimization (ACO) [14], and reinforcement learning [19].

EETT aims to generate a timetable of one or multiple trains that has the lowest total energy consumption by determining the optimal distribution of running time supplements [20], [21] or headway between consecutive trains [22], [23]. Since energy consumption and travel time are contradictory objectives, EETT has to make a trade-off between them. The energy-efficient timetable determined by an EETT method is provided to the EETC. However, when train traffic is perturbed, conflicts between trains may arise. In this case, the trains must be rerouted, reordered, and rescheduled; hence, the original timetable is recalculated. This problem, the so-called real-time railway traffic management problem (rtRTMP) [24], has been tackled by much research, as [25]–[27]. However, rtRTMP optimization models usually focus on train delays and neglect energy optimization. Models that tackle this real-time energy consumption minimization problem (rtECMP) [28] already exist. Montrone et al. proposed a mixed integer linear programming model in [28] to find energy-efficient driving regimes after solving the rtRTMP. Naldini et al. reformulated the problem with a graph-based model solved by ant colony optimization [29]. Su et al. proposed a method that can calculate an energy-optimal speed profile in real-time given a timetable and generate an integrated optimal timetable [30]. However, [30] does not consider the influence of multiple trains on each other as [28], [29]. The integrated optimization of the central traffic management system (TMS) that solves the rtRTMP and automatic train operation (ATO) generating energy-efficient speed profiles is presented in [31], [32].

In this paper, we propose a non-linear optimization model that tackles the real-time energy consumption minimization problem, calculating energy-efficient speed profiles. The rest of the paper is organized as follows. The problem is described in detail in Section II. The formulation of the proposed optimization model is given in Section III. The experimental results, along with the evaluation methodology and experimental setup, are presented in Section IV. Finally, the conclusions are drawn with a brief outlook on the future works in Section V.

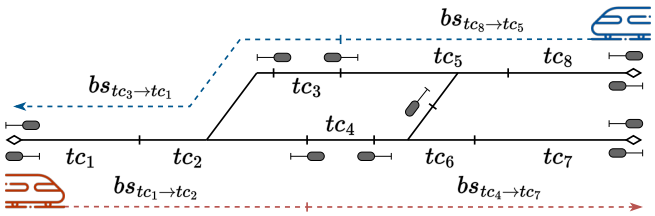

Fig. 1: The two-level real-time energy optimization workflow

II. Problem Description

Railway networks are split into disjoint control areas managed by dispatchers. An example of a simplified control area is illustrated in Fig. 1. The control area can be modeled as a graph network whose edges are grouped to track circuits denoted by tc, where the presence of a train is automatically detected. The block sections, denoted by bs, are formed by a group of track circuits delimited by signals at their entry and exit locations. It should be noted that track circuits can belong to multiple block sections according to the different routes and directions. In the example in Fig. 1, tc_1 belongs both to $bs_{tc_3 \to tc_1}$ and $bs_{tc_1 \to tc_2}$ along the blue and red train routes, respectively. The routes are composed of the consecutive order of block sections. When a train approaches a signal, the subsequent block section's track circuits are reserved before the train enters the block section, considering a time buffer called formation time. For the sake of simplicity, we consider a signaling system with two aspects: red and green. In a three-aspect signaling system, two consecutive block sections are kept clear for a train. The reservation of a track circuit is finished shortly after the train exits the block section, considering the release time of the interlocking system. A track circuit cannot be reserved simultaneously by multiple trains. Therefore, block sections with common track circuits, as $bs_{tc_3 \to tc_1}$ and $bs_{tc_1 \to tc_2}$ in Fig. 1, can also be reserved by at most one train at a given time.

The original timetable is designed by considering these traffic regulations to let traffic operate smoothly. The real-time railway traffic management problem (rtRTMP) occurs when railway traffic is perturbed, causing primary train delays. The trains must be rerouted, reordered, and rescheduled to avoid conflicts, considering the regulations above. Since most of the optimization models focus on minimizing the secondary delays that have to be assigned to trains to solve the rtRTMP, the real-time energy consumption minimization problem (rtECMP) is usually tackled after the rtRTMP, forming a two-level optimization illustrated in Fig. 2. The first level is not a subject of this paper; we used one of the state-of-the-art MILP models [24] to tackle it. Then, the routing and the precedence between the trains are provided to the second level, the real-time energy consumption minimization problem. We propose a non-linear model for this problem, which determines an energy-efficient velocity profile and creates and reschedules the trains accordingly, creating a new integrated timetable.

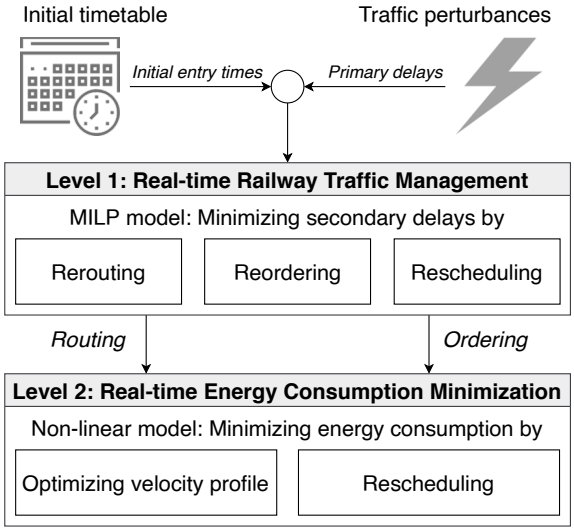

Fig. 2: The two-level real-time energy optimization workflow

III. Model formulation

The optimization goal is to determine a velocity profile for each train along their route that minimizes energy consumption. The routing and precedence between the trains are provided by the traffic management, as seen in Fig. 2. Since the sequence of block sections forms the train route, it makes sense to calculate the speed profile in sections according to them. However, speed restrictions may occur even within block sections. The block sections must be split into subsections. For the sake of simplicity, we defined the speed limits with respect to the track circuits. Therefore, the speed profile is also given concerning the track circuits. However, it should be noted that speed restrictions usually arise less frequently in practice, and determining the speed in each track circuit can be computationally demanding in extensive networks. Moreover, each track circuit is divided into three partitions corresponding to the maximum acceleration, deceleration, and cruising driving regimes. Indeed, according to [8], there is an additional optimal driving regime, the coasting. However, according to our previous experiments, neglecting the coasting does not significantly impact the results, but it is reasonable due to computational complexity. Therefore, the V_i velocity profile of train i is formulated as

$$V_i = \left[v_{i,j}\right] \quad j = 1, \ldots, 2 \times |S_i| + 1\,, \tag{1}$$

where S_i denotes the subsections the route of train i is divided into, which are now identical to the track circuits, and $|S_i|$ is the cardinality of S_i. The velocity profile of a subsection, $s_k \in S_i$ $(k = 1, \ldots, |S_i|)$, can be described by v_{i,s_k}^{start}, v_{i,s_k}^{end} and v_{i,s_k}^{mid}, corresponding to the starting, ending, and cruising velocities derived from the overall velocity profile as

$$\begin{aligned} v_{i,s_k}^{\text{start}} &= v_{i,2(k-1)+1}\,, \\ v_{i,s_k}^{\text{mid}} &= v_{i,2(k-1)+2}\,, \\ v_{i,s_k}^{\text{end}} &= v_{i,2(k-1)+3}\,. \end{aligned} \tag{2}$$

An example of such a velocity profile is illustrated in Fig. 3, which consists of 4 subsections, resulting in a velocity profile of 9 elements. For the sake of visibility, the velocity profile is only connected with subsection s_1 in Fig. 3; however, it can be easily given for further ones using (2). Moreover, the index i of the train is omitted. It can be seen that the subsections do not necessarily have all three different driving regimes, only a subset of them. If the speed limit of a subsection is lower than that of the preceding one (e.g., from s_1 to s_2), the velocity must be reduced before entering it. If a block section has a higher speed limit than the preceding one (e.g., from s_2 to s_3), the acceleration can only be started after entering it. Indeed, the maximum acceleration varies with speed in hyperbolic form. However, we neglect this, supposing a constant acceleration and deceleration, as illustrated in Fig. 3. Based on previous experiments, we believe this assumption does not significantly impair the model. Then, the t^{part}_{i,s_k} duration and d^{part}_{i,s_k} travel distance of the velocity profile partitions ($\text{part} \in \{\text{start}, \text{mid}, \text{end}\}$) of train i in subsection s_k according to the driving regimes can be computed by the following kinematic equations:

$$t^{\text{start}}_{i,s_k} = \begin{cases} \dfrac{v^{\text{mid}}_{i,s_k} - v^{\text{start}}_{i,s_k}}{a^{\text{acc}}_i} & \text{if } v^{\text{mid}}_{i,s_k} > v^{\text{start}}_{i,s_k} \text{ (accel.)} \\ \dfrac{v^{\text{start}}_{i,s_k} - v^{\text{mid}}_{i,s_k}}{a^{\text{dec}}_i} & \text{otherwise (decel.)} \end{cases} \tag{3}$$

$$t^{\text{end}}_{i,s_k} = \begin{cases} \dfrac{v^{\text{end}}_{i,s_k} - v^{\text{mid}}_{i,s_k}}{a^{\text{acc}}_i} & \text{if } v^{\text{end}}_{i,s_k} > v^{\text{mid}}_{i,s_k} \text{ (accel.)} \\ \dfrac{v^{\text{mid}}_{i,s_k} - v^{\text{end}}_{i,s_k}}{a^{\text{dec}}_i} & \text{otherwise (decel.)} \end{cases} \tag{4}$$

$$t^{\text{mid}}_{i,s_k} = \frac{d^{\text{mid}}_{i,s_k}}{v^{\text{mid}}_{i,s_k}} \quad \text{(cruising)} \tag{5}$$

$$d^{\text{start}}_{i,s_k} = \begin{cases} \dfrac{\left(v^{\text{mid}}_{i,s_k}\right)^2 - \left(v^{\text{start}}_{i,s_k}\right)^2}{2a^{\text{acc}}_i} & \text{if } v^{\text{mid}}_{i,s_k} > v^{\text{start}}_{i,s_k} \text{ (accel.)} \\ \dfrac{\left(v^{\text{start}}_{i,s_k}\right)^2 - \left(v^{\text{mid}}_{i,s_k}\right)^2}{2a^{\text{dec}}_i} & \text{otherwise (decel.)} \end{cases} \tag{6}$$

$$d^{\text{end}}_{i,s_k} = \begin{cases} \dfrac{\left(v^{\text{end}}_{i,s_k}\right)^2 - \left(v^{\text{mid}}_{i,s_k}\right)^2}{2a^{\text{acc}}_i} & \text{if } v^{\text{end}}_{i,s_k} > v^{\text{mid}}_{i,s_k} \text{ (accel.)} \\ \dfrac{\left(v^{\text{mid}}_{i,s_k}\right)^2 - \left(v^{\text{end}}_{i,s_k}\right)^2}{2a^{\text{dec}}_i} & \text{otherwise (decel.)} \end{cases} \tag{7}$$

$$d^{\text{mid}}_{i,s_k} = d_{s_k} - d^{\text{start}}_{i,s_k} - d^{\text{end}}_{i,s_k} \quad \text{(cruising)} \tag{8}$$

where a^{acc}_i and a^{dec}_i denote the maximum acceleration and deceleration of train i, and d_{s_k} is the total length of subsection s_k. The partitions 'start' and 'end' of t_{i,s_k} and d_{i,s_k} connect v^{start}_{i,s_k} with v^{mid}_{i,s_k} and v^{mid}_{i,s_k} with v^{end}_{i,s_k}, respectively. If a subsection does not include all three driving regimes, the t duration and d length of the corresponding partition (start or end) is zero. The t_{i,s_k} total running time of train i on subsection s_k is computed by the sum of the t^{start}_{i,s_k}, t^{mid}_{i,s_k}, t^{end}_{i,s_k} partitions.

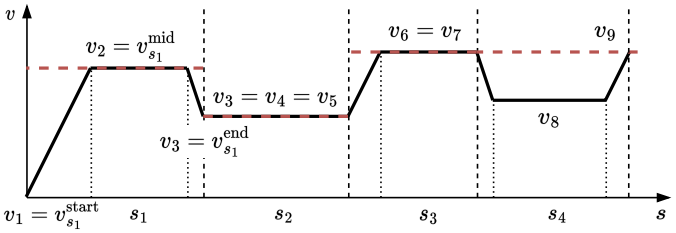

Fig. 3: Illustration of a velocity profile in which the dashed and dotted lines represent the limits of the subsections and driving regime partitions, respectively. The red dashed lines illustrate the speed limit of the corresponding subsection.

The energy consumption of a partition with v_0 starting and v_1 ending velocity and d travel distance can be computed as

$$E(v_0, v_1, d) = E_{\text{acc}}(v_0, v_1) + E_{\text{res}}(v_0, v_1, d)\,, \tag{9}$$

where E_{res} and E_{acc} denote the energy consumption due to the propulsion resistance and acceleration. The energy consumption, E_{acc}, can be given by the change in kinetic energy in an acceleration phase, and 0 otherwise:

$$E_{\text{acc}} = \begin{cases} \dfrac{m(v_1^2 - v_0^2)}{2} & \text{if } v_1 > v_0 \\ 0 & \text{otherwise} \end{cases}, \tag{10}$$

where m denotes the mass of the train. The energy consumption due to the F_{res} resistance force is computed as

$$E_{\text{res}} = \begin{cases} \displaystyle\int_0^d F_{\text{res}}(v(s))\,\mathrm{d}s & \text{if } v_1 \geq v_0 \\ 0 & \text{otherwise,} \end{cases} \tag{11}$$

where d denotes the length of the corresponding partition between v_0 and v_1. The resistance force is given depending on the v velocity according to the Davies equation as

$$F_{\text{res}} = \alpha + \beta v + \gamma v^2\,, \tag{12}$$

where α, β, and γ are the propulsion resistance coefficients. In cruising phases, the integral in (11) simply results in

$$E^{\text{cruise}}_{\text{res}} = (\alpha + \beta v_0 + \gamma v_0^2)\,d\,. \tag{13}$$

The resistance force $F^{\text{acc}}_{\text{res}}$ during an acceleration phase can be expressed with the travel distance, s, by simply substituting $v(s) = \sqrt{2a^{\text{acc}}s + v_0^2}$ into (12) as follows:

$$F^{\text{acc}}_{\text{res}}(s) = \alpha + \beta\sqrt{2a^{\text{acc}}s + v_0^2} + \gamma(2a^{\text{acc}}s + v_0^2)\,. \tag{14}$$

Since the effect of $\beta \approx 0$ is often neglected in practice, the energy consumption due to resistance during acceleration is

$$E^{\text{acc}}_{\text{res}} \approx (\alpha + \gamma a^{\text{acc}} d + \gamma v_0^2)\,d\,. \tag{15}$$

So, the generic definition of the E_{res} energy consumption in (9) due to propulsion resistance is given as

$$E_{\text{res}} = \begin{cases} (\alpha + \gamma v_0^2)\,d & \text{if } v_1 = v_0 \\ (\alpha + \gamma a^{\text{acc}} d + \gamma v_0^2)\,d & \text{if } v_1 > v_0 \\ 0 & \text{otherwise} \end{cases}. \tag{16}$$

Then, the E^{part}_{i,s_k} energy consumed during the velocity profile partitions ($\text{part} \in \{\text{start}, \text{mid}, \text{end}\}$) of train i in subsection s_k is given relying on (9) as

$$E^{\text{start}}_{i,s_k} = E(v^{\text{start}}_{i,s_k}, v^{\text{mid}}_{i,s_k}, d^{\text{start}}_{i,s_k}) \,, \tag{17}$$

$$E^{\text{mid}}_{i,s_k} = E(v^{\text{mid}}_{i,s_k}, v^{\text{mid}}_{i,s_k}, d^{\text{mid}}_{i,s_k}) \,, \tag{18}$$

$$E^{\text{end}}_{i,s_k} = E(v^{\text{mid}}_{i,s_k}, v^{\text{end}}_{i,s_k}, d^{\text{end}}_{i,s_k}) \,. \tag{19}$$

The optimization objective is given by the sum of the total energy consumption of each train i as

$$\min_{v_{i,j}} \sum_{\forall i \in T} \sum_{\forall s_k \in S_i} E^{\text{start}}_{i,s_k} + E^{\text{mid}}_{i,s_k} + E^{\text{end}}_{i,s_k} \,, \tag{20}$$

where T denotes the set of trains included in the rtECMP.

Indeed, a trade-off between the delays and energy consumption is usually considered in the objective function. However, we have found that defining this trade-off in the following constraint applied for each $i \in T$ provides more flexibility to the optimization algorithm:

$$\sum_{\forall s_k \in S_i} t^{\text{start}}_{i,s_k} + t^{\text{mid}}_{i,s_k} + t^{\text{end}}_{i,s_k} \leq w^{\text{del}}_i (exit_i - init_i) \,, \tag{21}$$

where $init_i$ and $exit_i$ denote the scheduled entry and exit time of train i, according to the solution of the traffic management problem, and $w^{\text{del}}_i > 1$ is the delay factor. The higher the factor is, the more delay is allowed for train i, contributing to a lower energy consumption. For example, $w^{\text{del}}_i = 1.1$ means that the total running time of the train can be 10% higher than it was planned. The new integrated timetable comprising the e_{i,s_k} times when train i enters the subsection s_k is:

$$e_{i,s_k} = e_{i,s_{k-1}} + t_{i,s_{k-1}} \,, \quad e_{i,s_1} = init_i, \tag{22}$$

According to the traffic regulations explained in Section II, a train i approaching a green signal reserves the whole block section before entering it. Let B_i denote the consecutive block sections $bs_l \in B_i$ ($l = 1, \ldots, |B_i|$) along the route of train i. A block section, bs_l, consists of one or more subsections as

$$bs_l = \begin{bmatrix} s^{bs_l}_1 & s^{bs_l}_2 & \ldots s^{bs_l}_{|bs_l|} \end{bmatrix} \tag{23}$$

Therefore, $sRes_{i,bs_l}$, denoting the time when train i starts reserving block section bs_l, is computed as

$$sRes_{i,bs_l} = e_{i,s_1^{bs_l}} - for \,, \tag{24}$$

considering the formation time by for and $s_1^{bs_l}$ denotes the first subsection of the block section bs_l as seen in (23). The block section is released shortly after the train leaves it. So, the reservation of block section bs_l is finished at

$$eRes_{i,bs_l} = e_{i,s_1^{bs_{l+1}}} + cl_{i,bs_l} + rel \,, \tag{25}$$

considering the rel release time and the cl_{s_k} clearing time while the train has already entered the subsequent block section bs_{l+1} but not wholly left bs_l. Finally, if train i' has precedence over train i ($i' \prec i$) according to the solution of the traffic management problem, train i cannot start reserving a block section $bs_l \in B_i$ that shares some track circuits with $bs'_l \in B_{i'}$ until train i' releases bs'_l:

$$sRes_{i,bs_l} \geq eRes_{i',bs'_l} \quad \forall i' \prec i, bs_l \cap bs'_l \neq \emptyset \tag{26}$$

IV. Experimental Analysis

The proposed methodology is evaluated experimentally via simulation. The simulation environment, along with other experimental setups, is detailed in Section IV-A. The implementation details are given in Section IV-B, and the evaluation results are shown in Section IV-C.

A. Experimental Setup

The experiments comprise two traffic scenarios in two different control areas, illustrated in Fig. 4. The first scenario includes three trains on a control area representing three stations connected by single line sections, as shown in Fig. 4a. The control area consists of 17 track circuits forming 8 routes. The track circuits containing the platforms (tc_2, tc_3, tc_7, tc_8, tc_{14}, tc_{15}) and switches (tc_1, tc_4, tc_6, tc_9, tc_{13}, tc_{16}) are equally 400 and 200 m long. While tc_5, tc_{10}, tc_{11}, and tc_{12} are 5000, 3000, 4000, and 3000 m long. There are multiple speed restrictions along the different routes. The route selection of the trains according to the solution of the traffic management problem is also shown in Fig. 4a. Trains 1 and 2 enter the control area simultaneously, while train 3 shortly after them. According to the traffic management system, train 1 has to wait for train 2 since having precedence at track circuit tc_7. Train 3 waits for train 1 first at track circuit tc_2 and then at tc_7. Meanwhile, train 2 has to wait for train 1 to pass tc_6.

The second scenario illustrated in Fig. 4b consists of four trains. The control area represents a three-line station with four entry and exit lines comprising 17 track circuits and 12 routes. The entry track circuits (tc_1, tc_2, tc_{16}, tc_{17}) are 3000 m long, followed by a 100 m long overlap (tc_3, tc_4, tc_{14}, tc_{15}). The track circuits containing the switches (tc_5, tc_6, tc_7, tc_{11}, tc_{12}, tc_{13}) are 600 and 700 m long on the straight and detour sections. The platforms illustrated by the dashed lines are 600 m long. The speed limit of the control area is 100 km/h except for the platforms and the detour track circuits, where there is a 50 km/h restriction. The route selection of the trains provided by the traffic management system is also illustrated in Fig. 4b. Each train enters the control area simultaneously. Train 1 and train 3 have precedence over train 2 and train 3, making them wait at track circuit tc_2 and tc_{16}. Then, train 3 waits for train 1 and train 2 to leave track circuits tc_7 and tc_6.

The trains are identically capable of a 100 km/h maximal speed, 0.4 m/s^2 acceleration, and 1.1 m/s^2 deceleration. The parameters of the Davies equation can be given by the m train mass as in [33]. Hence, α and γ parameters in (16) as

$$\alpha = 2 \times 2.725 \times 10^{-9} m \,, \tag{27}$$

$$\gamma = 7.76952 \times 10^{-12} m \,, \tag{28}$$

neglecting the effect of β, where m is set at 150 t identically for each train. First, an initial optimization is executed, minimizing train delays compared to the rescheduled timetable provided by the traffic management system to determine the fastest velocity profile. Then, the energy optimization is performed with two w^{del} delay factor settings: a moderate one enabling 5% delay ($w^{\text{del}} = 1.05$) and a more permissive one with a 10% maximal delay ($w^{\text{del}} = 1.10$).

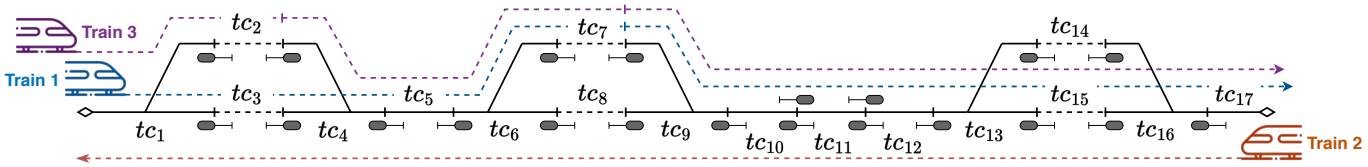

(a) Scenario 1

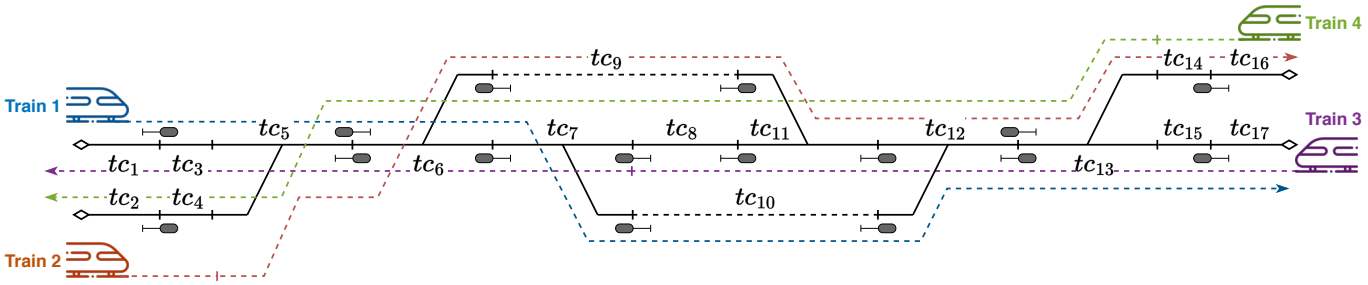

(b) Scenario 2

Fig. 4: Illustration of evaluation scenarios

B. Implementation Details

Besides the velocity profile defined in (1), the x optimization state-space includes the t^{part}_{i,s_k} duration of partitions, e_{i,s_k} entry times, and $sRes_{i,bs_l}$, $eRes_{i,bs_l}$ reservation times as:

$$x = \left[v_{i,j} \quad t^{\text{start}}_{i,s_k} \quad t^{\text{mid}}_{i,s_k} \quad t^{\text{end}}_{i,s_k} \quad e_{i,s_k} \quad sRes_{i,bs_l} \quad eRes_{i,bs_l}\right]^\top,$$
$$\forall i \in T, j \in \{1, \dots, 2 \times |S_i| + 1\}, s_k \in S_i, bs_l \in B_i \quad (29)$$

The lower boundary of each state is zero, and the upper boundaries of $v_{i,j}$ elements are set according to the speed limits. The t^{part}_{i,s_k} duration of the partitions in (3)-(5) are given with nonlinear constraints. While the expressions in (21)-(22) and (24)-(26) can be given by linear constraints. Finally, the objective function in (20) is also defined by a nonlinear expression.

The optimization problem is solved with the `fmincon` function of Matlab Optimization Toolbox relying on the interior-point method. The experiments are performed on a Lenovo ThinkCentre PC with Intel Core i7-10700 CPU @2.9 GHz, 2 cores, and 16 GB RAM in Matlab R2021b.

C. Results

The results of the two scenarios are given in Table I and Table II while the velocity profiles along with the evolution of energy consumption over the traveled distance are shown in Fig. 5 and Fig. 6. In the first scenario illustrated in Fig. 4a, the three trains consume 12.79%, 11.22%, and 23.27% less energy due to energy optimization with a 5% maximal additional delay. Therefore, the overall energy consumption is reduced by 16.33% compared to the fastest velocity profile. Moreover, enabling a 10% maximal delay gains 7.45% more energy consumption reduction. As seen in Fig. 5, the key to energy efficiency is avoiding significant velocity changes. Therefore, energy optimization tries to keep trains from stopping and reducing the speed in advance before the train must reduce the speed significantly. Despite the lower energy consumption of the fastest velocity profile because of the smaller control area of the second scenario seen in Fig. 4b, the energy consumption

TABLE I: Resulting delay and energy consumption of 1st scenario according to the different methods (RTO - running time optimal, $EO_{5\%}$ - moderate energy optimal with $w^{\text{del}} = 1.05$, $EO_{10\%}$ - permissive energy optimal with $w^{\text{del}} = 1.10$)

	Delay [s]			Energy consumption [kWh]		
	RTO	$EO_{5\%}$	$EO_{10\%}$	RTO	$EO_{5\%}$	$EO_{10\%}$
Train 1	0.30	34.67	72.86	50.48	44.02	41.26
Train 2	2.62	37.86	73.08	49.48	43.93	40.94
Train 3	0.30	51.72	103.13	62.13	47.67	43.32
Total	3.22	124.25	249.07	162.09	135.62	125.52

TABLE II: Resulting delay and energy consumption of 2nd scenario according to the different methods (RTO - running time optimal, $EO_{5\%}$ - moderate energy optimal with $w^{\text{del}} = 1.05$, $EO_{10\%}$ - permissive energy optimal with $w^{\text{del}} = 1.10$)

	Delay [s]			Energy consumption [kWh]		
	RTO	$EO_{5\%}$	$EO_{10\%}$	RTO	$EO_{5\%}$	$EO_{10\%}$
Train 1	0.09	21.26	42.43	34.60	26.35	26.96
Train 2	0.03	25.67	51.31	41.80	24.93	24.07
Train 3	0.46	20.80	41.14	32.61	28.33	22.44
Train 4	0.48	24.12	47.77	50.48	27.02	27.14
Total	1.06	91.85	182.65	159.49	106.63	100.61

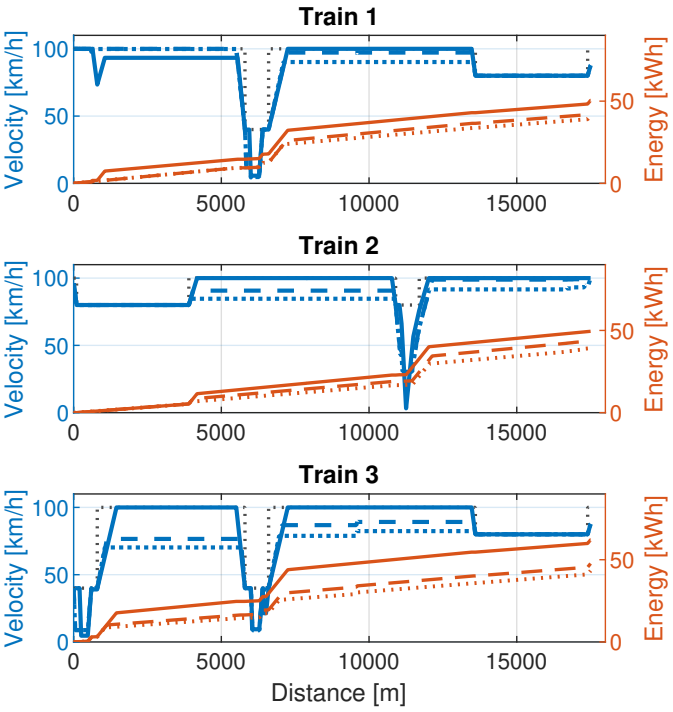

Fig. 5: The velocity profiles and resulting energy consumption curves of trains in the 1st scenario, where the solid, dashed, and dotted lines correspond to the fastest, moderate-, and permissive energy-efficient solutions. The black dotted lines denote the speed limits.

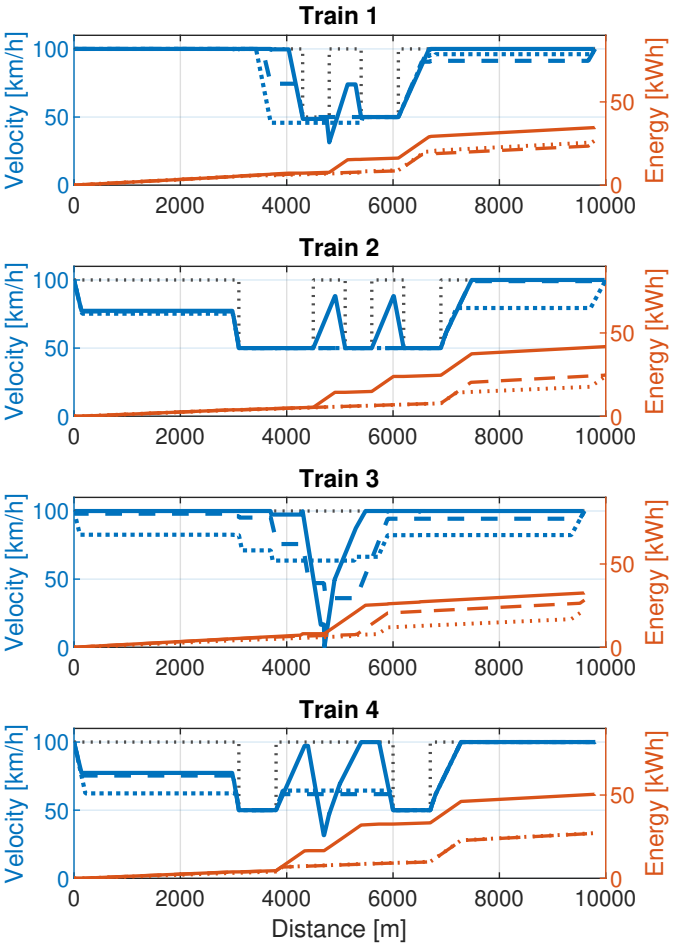

Fig. 6: The velocity profiles and resulting energy consumption curves of trains in the 2nd scenario, where the solid, dashed, and dotted lines correspond to the fastest, moderate-, and permissive energy-efficient solutions. The black dotted lines denote the speed limits.

reduction of the optimization is even more significant. The energy-efficient velocity profile with a 5% maximal delay reduced the energy consumption by 23.84%, 40.36%, 13.12%, and 46.47% of the four trains, resulting in a 33.14% lower overall energy consumption compared to the faster velocity profile. The most significant reduction is achieved by train 2 and train 4, to which the traffic management system assigns the lowest delays; therefore, these trains have the most potential to reduce their energy consumption by smoothing the peaks of the fastest velocity profile, as seen in Fig. 4b. However, in the second scenario, there is no significant difference between moderate ($w^{\mathrm{del}} = 1.05$) and permissive ($w^{\mathrm{del}} = 1.10$) energy optimization, unlike in the first one, since only train 3 can decrease its energy consumption by a further 20.79%.

V. Conclusions and Future Works

This paper presented a two-level workflow for the real-time railway energy consumption minimization problem. The first level can use any state-of-the-art solver to tackle the real-time traffic management problem. For the second level, we propose a nonlinear optimization model to minimize the energy consumption of the trains, considering the route selection and precedence between trains determined in the first level. Instead of choosing the combination of the driving regimes, the proposed model directly determines an energy-efficient velocity profile for each train, relying on a simplified train model assuming constant acceleration and deceleration. The energy-efficient speed profiles reduce energy consumption by ∼15-25% depending on the scenario and the maximum delay allowed. As a part of future work, we want to extend the proposed model by considering the planned dwell times of the trains. Moreover, we plan to perform a more detailed analysis of the proposed workflow in more realistic large networks.

Acknowledgment

The research was supported by the European Union within the framework of the National Laboratory for Autonomous Systems. (RRF-2.3.1-21-2022-00002)
This work was partially supported by the János Bolyai Research Scholarship of the Hungarian Academy of Sciences.
The project is also supported by the New National Excellence Program of the Ministry for Innovation and Technology from the Source of the National Research, Development and Innovation Fund, under Grant ÚNKP-23-3.

REFERENCES

[1] T. Skrucany, M. Kendra, M. Skorupa, J. Grencik, and T. Figlus, "Comparison of chosen environmental aspects in individual road transport and railway passenger transport," *Procedia Engineering*, vol. 192, pp. 806–811, 2017, 12th international scientific conference of young scientists on sustainable, modern and safe transport. [Online]. Available: https://www.sciencedirect.com/science/article/pii/S1877705817326863

[2] S. Ribeiro, M. Figueroa, F. Creutzig, C. Dubeux, J. Hupe, and S. Kobayashi, *Global Energy Assessment - Toward a Sustainable Future. Chapter 9 - Energy End-Use: Transport*, 06 2012.

[3] D. M. Z. Islam, R. Jackson, T. H. Zunder, and A. Burgess, "Assessing the impact of the 2011 eu transport white paper-a rail freight demand forecast up to 2050 for the eu27," *European Transport Research Review*, vol. 7, no. 3, pp. 1–9, 2015.

[4] C. Filippi, G. Guastaroba, L. Peirano, and M. G. Speranza, "Trends in passenger transport optimisation," *International Transactions in Operational Research*, 2023.

[5] A. García-Olivares, J. Solé, and O. Osychenko, "Transportation in a 100% renewable energy system," *Energy Conversion and Management*, vol. 158, pp. 266–285, 2018. [Online]. Available: https://www.sciencedirect.com/science/article/pii/S0196890417312050

[6] P. M. Fernández, I. V. Sanchís, V. Yepes, and R. I. Franco, "A review of modelling and optimisation methods applied to railways energy consumption," *Journal of Cleaner Production*, vol. 222, pp. 153–162, 2019.

[7] G. M. Scheepmaker, R. M. Goverde, and L. G. Kroon, "Review of energy-efficient train control and timetabling," *European Journal of Operational Research*, vol. 257, no. 2, pp. 355–376, 2017.

[8] M. Miyatake and H. Ko, "Optimization of train speed profile for minimum energy consumption," *IEEJ Transactions on Electrical and Electronic Engineering*, vol. 5, no. 3, pp. 263–269, 2010.

[9] A. Albrecht, P. Howlett, P. Pudney, X. Vu, and P. Zhou, "The key principles of optimal train control—part 1: Formulation of the model, strategies of optimal type, evolutionary lines, location of optimal switching points," *Transportation Research Part B: Methodological*, vol. 94, pp. 482–508, 2016.

[10] ——, "The key principles of optimal train control—part 2: Existence of an optimal strategy, the local energy minimization principle, uniqueness, computational techniques," *Transportation Research Part B: Methodological*, vol. 94, pp. 509–538, 2016.

[11] Y. Bocharnikov, A. M. Tobias, and C. Roberts, "Reduction of train and net energy consumption using genetic algorithms for trajectory optimisation," in *IET Conference on Railway Traction Systems (RTS 2010)*, 2010, pp. 1–5.

[12] M. Domínguez, A. Fernández, A. Cucala, and P. Lukaszewicz, "Optimal design of metro automatic train operation speed profiles for reducing energy consumption," *Proceedings of the Institution of Mechanical Engineers, Part F: Journal of Rail and Rapid Transit*, vol. 225, no. 5, pp. 463–474, 2011.

[13] A. Fernandez-Rodriguez, A. Fernández-Cardador, A. P. Cucala, M. Domínguez, and T. Gonsalves, "Design of robust and energy-efficient ato speed profiles of metropolitan lines considering train load variations and delays," *IEEE Transactions on Intelligent Transportation Systems*, vol. 16, no. 4, pp. 2061–2071, 2015.

[14] N. Zhao, C. Roberts, S. Hillmansen, and G. Nicholson, "A multiple train trajectory optimization to minimize energy consumption and delay," *IEEE Transactions on Intelligent Transportation Systems*, vol. 16, no. 5, pp. 2363–2372, 2015.

[15] P. G. Howlett, P. J. Pudney, and X. Vu, "Local energy minimization in optimal train control," *Automatica*, vol. 45, no. 11, pp. 2692–2698, 2009.

[16] E. Khmelnitsky, "On an optimal control problem of train operation," *IEEE transactions on automatic control*, vol. 45, no. 7, pp. 1257–1266, 2000.

[17] S. Lu, M. Q. Wang, P. Weston, S. Chen, and J. Yang, "Partial train speed trajectory optimization using mixed-integer linear programming," *IEEE Transactions on Intelligent Transportation Systems*, vol. 17, no. 10, pp. 2911–2920, 2016.

[18] S. Ahmadi, A. Dastfan, and M. Assili, "Energy saving in metro systems: Simultaneous optimization of stationary energy storage systems and speed profiles," *Journal of rail transport planning & management*, vol. 8, no. 1, pp. 78–90, 2018.

[19] M. A. Sandidzadeh and P. Havaei, "A comprehensive study on reinforcement learning application for train speed profile optimization," *Multimedia Tools and Applications*, vol. 82, no. 24, pp. 37 351–37 386, Oct 2023.

[20] T. Albrecht and S. Oettich, "A new integrated approach to dynamic schedule synchronization and energy-saving train control," *WIT Transactions on The Built Environment*, vol. 61, 2002.

[21] S. Su, X. Li, T. Tang, and Z. Gao, "A subway train timetable optimization approach based on energy-efficient operation strategy," *IEEE transactions on intelligent transportation systems*, vol. 14, no. 2, pp. 883–893, 2013.

[22] Y. Wang, B. De Schutter, T. J. van den Boom, and B. Ning, "Optimal trajectory planning for trains under fixed and moving signaling systems using mixed integer linear programming," *Control Engineering Practice*, vol. 22, pp. 44–56, 2014.

[23] P. Wang, R. M. Goverde, and L. Ma, "A multiple-phase train trajectory optimization method under real-time rail traffic management," in *2015 IEEE 18th International Conference on Intelligent Transportation Systems*. IEEE, 2015, pp. 771–776.

[24] P. Pellegrini, G. Marlière, and J. Rodriguez, "Optimal train routing and scheduling for managing traffic perturbations in complex junctions," *Transportation Research Part B: Methodological*, vol. 59, pp. 58–80, 2014.

[25] A. D'Ariano, F. Corman, D. Pacciarelli, and M. Pranzo, "Reordering and local rerouting strategies to manage train traffic in real time," *Transportation science*, vol. 42, no. 4, pp. 405–419, 2008.

[26] F. Corman, A. D'Ariano, D. Pacciarelli, and M. Pranzo, "A tabu search algorithm for rerouting trains during rail operations," *Transportation Research Part B: Methodological*, vol. 44, no. 1, pp. 175–192, 2010.

[27] P. Pellegrini, G. Marlière, R. Pesenti, and J. Rodriguez, "Recife-milp: An effective milp-based heuristic for the real-time railway traffic management problem," *IEEE Transactions on Intelligent Transportation Systems*, vol. 16, no. 5, pp. 2609–2619, 2015.

[28] T. Montrone, P. Pellegrini, and P. Nobili, "Real-time energy consumption minimization in railway networks," *Transportation Research Part D: Transport and Environment*, vol. 65, pp. 524–539, 2018.

[29] F. Naldini, P. Pellegrini, and J. Rodriguez, "Real-time optimization of energy consumption in railway networks," *Transportation Research Procedia*, vol. 62, pp. 35–42, 2022.

[30] S. Su, X. Li, T. Tang, and Z. Gao, "A subway train timetable optimization approach based on energy-efficient operation strategy," *IEEE Transactions on Intelligent Transportation Systems*, vol. 14, no. 2, pp. 883–893, 2013.

[31] X. Rao, M. Montigel, and U. Weidmann, "Holistic optimization of train traffic by integration of automatic train operation with centralized train management," *Computers in Railways XIII: Computer System Design and Operation in the Railway and Other Transit Systems (Wit Transactions on the Built Environment)*, vol. 127, pp. 39–50, 2013.

[32] ——, "A new rail optimisation model by integration of traffic management and train automation," *Transportation Research Part C: Emerging Technologies*, vol. 71, pp. 382–405, 2016.

[33] S. Aradi, "Application of vehicle-to-infrastucture networks in vehicle control and monitoring system," Ph.D. dissertation, Budapesti Műszaki és Gazdaságtudományi Egyetem, 2015.